Journal of Organometallic Chemistry 883 (2019) 25–34

Contents lists available at ScienceDirect

Journal of Organometallic Chemistry

journal homepage: www.elsevier.com/locate/jorganchem

Hydrogenation of CO_2, carbonyl and imine substrates catalyzed by [IrH_3($^{Ph}PN^HP$)] complex

Ayyappan Ramaraj, Munirathinam Nethaji, Balaji R. Jagirdar*

Department of Inorganic & Physical Chemistry, Indian Institute of Science, Bangalore 560012, India

ARTICLE INFO

Article history:
Received 2 November 2018
Received in revised form
25 December 2018
Accepted 26 December 2018
Available online 31 December 2018

Keywords:
Pincer ligand
Iridium complexes
NMR spectroscopy
CO_2 activation
Hydrogenation
Catalysis

ABSTRACT

A series of iridium and rhodium complexes [M(COD)($^{Ph}PN^HP$)]Cl {M = Ir (**1**), Rh (**2**)}, [MH_2Cl($^{Ph}PN^HP$)] {M = Ir (**3**), Rh (**4**)} and [IrH_3($^{Ph}PN^HP$)] (**6**) supported by pincer ligand H–N($CH_2CH_2PPh_2$)$_2$ {$^{Ph}PN^HP$} have been synthesized and characterized. All complexes were isolated in good yields. The iridium trihydride complex [IrH_3($^{Ph}PN^HP$)] (**6**) was found to be an active catalyst for the hydrogenation of CO_2 in 1 M aqueous KOH solution. It also acts as a catalyst for the base-free hydrogenation of carbonyl and imine substrates in MeOH. Under similar hydrogenation conditions, 2-cyclohexen-1-one undergoes solvent assisted tandem Michael addition-reduction mediated by bifunctional Lewis-acid-catalyst [IrH_3($^{Ph}PN^HP$)] in ROH (R = Me, Et) at room temperature. The complexes **1, 3, 4,** and **6** were characterized by X-ray crystallography. Extensive hydrogen bonding interactions N–H···H–Ir (2.15 Å), N–H···Cl (2.370 Å) were noted in the crystal structures of these complexes.

1. Introduction

Significant research attention has been focused to develop methodologies which could bring down CO_2 levels in the atmosphere such that the hazards involved with global warming process could be curbed [1]. Currently, the majority of value-added chemicals are produced using CO as a C1 synthon which in turn is obtained by steam reforming of non-renewable, limited oil or natural gas resources. So in the last two decades, CO_2 has emerged as a front runner for an alternative, sustainable C1 feed-stock compared to fossil fuel sources. Parallelly, it must be noted that the effective utilization of CO_2 into value-added chemicals would critically depend on the production of H_2 from non-fossil fuel based energy sources like electrolysis of water, solar water splitting etc.

$$H_2 + CO_2 \xrightarrow{\text{catalyst}} HCOOH, CH_3OH$$

Among the different ways to utilize CO_2, approaches based on conversion of CO_2 into value added chemicals such as HCOOH, CH_3OH etc. using transition metal catalysts are being actively pursued (eq 1) [2,3]. In this context, transition metal complexes possessing multidentate pincer scaffold for the activation and functionalization of CO_2 has become increasingly prominent owing to their thermal stability, chelation rigidity and modulation of their electronic and steric properties [4]. The substituents on the pincer motif could readily be altered due to ease in synthesis and their catalytic activities could be evaluated. Thus, these ligands find applications in many areas such as hydrogenation, dehydrogenation, C–C coupling reactions, CO_2 activation and condensation reactions, etc. The most commonly employed pincer ligands relevant to the present work are shown in chart 1.

Among these, complexes with type (A) ligand H–N($CH_2CH_2PR_2$)$_2$ where R = isopropyl (^{i}Pr) substituent on phosphorus have been used for the activation of CO_2. Hazari and co-workers reported conversion of CO_2 into HCOOK using [IrH_3(HN($CH_2CH_2P^iPr_2$)$_2$)] {HN($CH_2CH_2P^iPr_2$)$_2$ = iPrPN^{H}P} complex as catalyst at 185 °C and 55 bar of total pressure (H_2 + CO_2) in the presence of 1 M aqueous KOH [5]. In addition to CO_2 activation, the transition metal complexes of ^{i}PrPN^{H}P ligand were used for the hydrogenation of carbonyl and imine substrates. Gusev et al. reported a series of metal hydride complexes such as *trans*-[ReH_2(NO)(^{i}PrPN^{H}P)], mer-[IrH_3(κ^3-PN^{H}N))] {PN^{H}N – tBu$_2$PC_2H_4NHC_2H_4NEt_2} and [IrH_3(^{i}PrPN^{H}P)] to be excellent catalysts for the hydrogenation of aldehydes, ketones, imines and α,β-unsaturated ketones, etc. [6] Hydrogenation of polar bonds such as those in carbonyl (R_2C = O) and imine (R_2C = N-R) moieties in organic substrates is an important reaction for the production of fine chemicals and building block

* Corresponding author.
E-mail address: jagirdar@iisc.ac.in (B.R. Jagirdar).

https://doi.org/10.1016/j.jorganchem.2018.12.017
0022-328X/

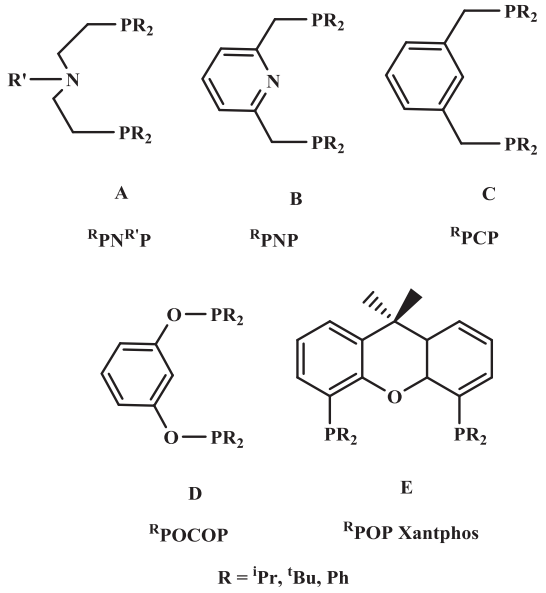

Chart 1. The most commonly employed pincer ligands relevant to the present work are shown.

reagents such as alcohols and amines respectively in pharmaceutical, fragrance and agricultural industry [7]. Direct hydrogenation in the presence of catalyst avoids the use of handling of stoichiometric, hazardous and air-sensitive reducing agents like $NaBH_4$ and $LiAlH_4$ and the subsequent waste generated after the workup [8,9].

Presence of different substituents in RPNHP (R = ^{i}Pr, *t*Bu, Ph) ligand could alter the electronic and steric profile at the metal center upon complexation. For example, Heinekey et al. studied the effect of substituents in RPOCOP (R = ^{i}Pr, *t*Bu) pincer skeleton with iridium complexes and have shown a dramatic effect on solubility, steric hindrance of substituents and reactivity upon changing the substituents on the pincer phosphorus [10]. Though very few early reports were documented on hydrogenation of cyclohexene using four coordinate Ir and Rh complexes [MCl(L)] {L = $HN(CH_2CH_2PPh_2)_2$ ($^{Ph}PN^{H}P$), M = Ir, Rh} in mid 1980s, metal complexes of $^{Ph}PN^{H}P$ ligand remain largely unexplored and their synthetic routes and characterization, not well established. Indeed, the [$MH_2Cl(^{Ph}PN^{H}P)$] {M = Ir, Rh} complexes have been proposed as intermediates in the hydrogenation of cyclohexene using [MCl(L)] complexes under H_2 atmosphere based on IR spectroscopy [11]. Recently, during the preparation of this manuscript, Casado et al. reported the synthesis of an extremely air sensitive four coordinate iridium amido complex [$Ir(COE)(N(CH_2CH_2PPh_2)_2)$] and demonstrated its utility in hydroamination of activated alkenes with NH_3(g) and C–H activation of alkynes [12].

In the present work, we have explored the untapped complexation potential of $HN(CH_2CH_2PPh_2)_2$ ligand with $[M(COD)Cl]_2$ {M = Ir, Rh} precursor and investigated the potential of the resulting complexes in catalysis. During the course of study, a series of iridium and rhodium complexes, [$M(COD)(^{Ph}PN^{H}P)$]Cl {M = Ir (**1**), Rh (**2**)}, [$MH_2Cl(^{Ph}PN^{H}P)$] {M = Ir (**3**), Rh (**4**)} and [$IrH_3(^{Ph}PN^{H}P)$] (**6**) supported by $^{Ph}PN^{H}P$ pincer ligand has been synthesized and well characterized. Complexes **1**, **3**, **4**, and **6** were characterized by X-ray crystallography. The iridium trihydride complex [$IrH_3(^{Ph}PN^{H}P)$] (**6**) was found to be an active catalyst for the hydrogenation of CO_2, carbonyl, 2-cyclohexen-1-one, and imines substrates. The results will be discussed in this paper.

2. Experimental section

All reactions were carried out under N_2/Ar atmosphere using standard Schlenk techniques or nitrogen filled glove box unless otherwise stated [13]. All glasswares were dried at 403 K overnight before use. 1,4-Dioxane, *n*-hexane, and THF were dried over Na-benzophenone. MeOH was dried over Mg/I_2 [14]. The solvents were degassed for 10–15 min just before use. C_6D_6, 1,4-dioxane-d_8, THF-d_8, CD_2Cl_2 and $CDCl_3$ were purchased either from Sigma Aldrich or Cambridge Isotope Laboratories and used as received. NMR spectra were recorded using Avance Bruker NMR spectrometer. The spectrometer frequencies for ^{1}H, $^{31}P\{^{1}H\}$ and $^{13}C\{^{1}H\}$ nuclei are 400, 162, and 100 MHz, respectively. The ^{1}H and ^{13}C NMR spectral chemical shifts were referenced to the residual proton signal of the deuterated solvents. ^{31}P NMR spectra were referenced relative to 85% H_3PO_4 aqueous solution (external reference). FTIR spectra of powder samples were recorded using a Bruker ALPHA-P spectrometer. Mass spectra were recorded using Micromass Q-TOF (HRMS) spectrometer in the Department of Organic Chemistry, Indian Institute of Science (IISc), Bangalore. Elemental analyses were carried out on ThermoFinnigan Flash EA 1112 CHNS analyzer, in the Department of Organic Chemistry, IISc, Bangalore. GC-MS data were collected using Agilent model equipped with GC 7890 A and MS 5975c model in the division of biological sciences, Indian Institute of Science, Bangalore.

1,5-Cyclooctadiene (COD), cyclooctene (COE), $NaBPh_4$, KOtBu and $LiN(SiMe_3)_2$ were purchased from Sigma Aldrich and used as received. The compounds $[IrCl(COD)]_2$, $[IrCl(COE)_2]_2$, $[RhCl(COD)]_2$, $NaBAr_4F$ (BAr_4F = $B[3,5\text{-}(CF_3)_2C_6H_3]_4$), $HN(CH_2CH_2PPh_2)_2$ ($^{Ph}PN^{H}P$) and $Me–N(CH_2CH_2PPh_2)_2$ (PhPNMeP) were prepared according to literature procedures [15–18]. The imine compounds, N-benzylidene aniline and N-benzylidene benzylamine used for the hydrogenation reactions were synthesized using the Dean-Stark method [19]. High pressure experiments were carried out either using Parr 4590 series micro-reactor equipped with 4843 series temperature controller or a home-built Swagelok dual mode high pressure/high vacuum setup. The high purity grade gases (>99.9999%) such as H_2, CH_4, and CO_2 were purchased from Bhuruka Gases Ltd, Bangalore, India. All precautions were strictly adhered to while carrying out high pressure experiments.

^{1}H and ^{31}P NMR spectral data for complexes **1**–**7** have been summarized in Table 1. ^{13}C NMR spectral data for all the compounds have been deposited in the S.M.

2.1. Synthesis of [Ir(COD)($^{Ph}PN^{H}P$)]Cl (1)

$[IrCl(COD)]_2$ (0.200 g, 0.298 mmol) and $HN\text{-}(CH_2CH_2PPh_2)_2$ (0.263 g, 0.596 mmol) were stirred together in THF (50 mL) for 12 h at 298 K. Then the solution was concentrated to about 5 mL, addition of *n*–hexane gave a colorless precipitate which was washed further with *n*–hexane (3 × 10 mL). The compound was dried in vacuo. Complex **1** was isolated as a colorless solid. Yield: 86% (0.400 g).

2.1.1. Characterization details of [Ir(COD)($^{Ph}PN^{H}P$)]Cl (**1**)

IR (ν(NH)): 3370 cm−1. HRMS: *m*/*z* = 742.2288 [M]+ (calcd *m*/*z* for $C_{36}H_{41}IrNP_2$ = 742.2343).

Elemental analysis for $C_{44}H_{55}NO_2P_2ClIr$: Calcd: C, 57.47; H, 6.03; N, 1.52; Found: C, 57.37; H, 5.30; N, 1.64. Two molecules of THF were found by NMR spectroscopy.

2.2. Synthesis of [Rh(COD)($^{Ph}PN^{H}P$)]Cl (2)

The synthetic procedure of [$Rh(COD)(^{Ph}PN^{H}P$]Cl (**2**) is similar to that of complex **1** except that $[RhCl(COD)]_2$ (0.114 g, 0.231 mmol)

Table 1
^{1}H and ^{31}P NMR spectral data for complexes **1**–**7**.

Complex	^{1}H						^{31}P	
	Ir–H/Rh–H	*J* (Hz)	CH_2	L	N–H	Ph	PhPNHP	*J*(Rh–P)
[Ir($^{Ph}PN^{H}P$)(COD)]Cl (**1**) [a]	–	–	2.30–3.46 (m, 8H)	1.44 (8H) and 3.94 (br s, 4 H)	8.21 (br s, 1H)	7.10–7.58 (m, 20H)	15.00	–
[Rh($^{Ph}PN^{H}P$)(COD)]Cl (**2**) [a]	–	–	2.48–3.25 (m, 8H)	1.47 (8H) and 4.31 (br s, 4H)	8.74 (br s, 1H)	7.20–7.79 (m, 20H)	36.67 (d)	120
[$IrH_2Cl(^{Ph}PN^{H}P)$] (**3**)	−23.98 (td, 1H), −19.04 (td, 1H)	(H,P) = 16, (H,H) = 7.5 Hz	2.52–3.51 (m, 8H)	–	4.19 (t, 1H), J(H,H) = 10 Hz	7.36–7.90 (m, 20H)	26.31	–
[$RhH_2Cl(^{Ph}PN^{H}P)$] (**4**)	−18.74 (m, 1H), −14.86 (m, 1H)	(Rh,P) = 28, (H,P) = 16, (H,H) = 9 Hz	2.30–3.27 (m, 8H)	–	4.30 (t, 1H), J(H,H) = 10 Hz	7.32–7.87 (m, 20H)	49.89 (d)	120
[$IrH_2(^{Ph}PNP)$] (**5**)	−20.10 (t, 2H)	(H,P) = 9 Hz	2.69–3.49 (m, 8H)	–	–	7.01–8.09 (m, 20H)	53.89	
mer-[$IrH_3(^{Ph}PN^{H}P)$] (**6a**)	−19.30 (m, 1H), −10.87 (td, 1H), −10.65 (td, 1H)	(H,P) = 18.5, (H,H) = 5 Hz	2.12–2.63 (m, 8H)	–	6.31 (t, 1H)	6.75–8.33 (m, 20H)	32.18	–
fac-[$IrH_3(^{Ph}PN^{H}P)$] (**6b**)	−19.47 (m, 1H), −10.35 (dd, 2H)	(H,P_{trans}) = 126, (H,P_{cis}) = 21, (H,H) = 5 Hz	1.72–3.45 (m, 8H)	–	5.26 (m, 1H)	6.75–8.33 (m, 20H)	27.89 (s)	–
[$IrH_2(\eta1\text{-}O\text{–}C(O)H)(^{Ph}PN^{H}P)$] (**7**) [b]	−27.10 (m, 1H), 17.97 (m, 1H)	(H,P) = 13.5, (H,H) = 7 Hz	2.28–3.54 (m, 8H)	9.09 (t)	8.81 (br s, 1H)	7.32–7.95 (m, 20H)	31.63	–

[a] L = COD, [b] L = HCOO−: For complexes **1** and **3**, NMR spectra were recorded in $CDCl_3$. For complexes **2** and **7**, NMR spectra were acquired in THF-d_8. For complex **4**, NMR spectrum was acquired in 1,4-dioxane-d_8. For complexes **5**, and **6**, NMR spectra were collected in C_6D_6.

and HN-($CH_2CH_2PPh_2$)$_2$ (0.200 g, 0.462 mmol) were used as starting materials. The reaction was stirred for 2 h at 273 K under Ar atm. Complex **2** was isolated as a highly air-sensitive yellow solid upon washing with *n*-hexane. Yield: 91% (0.290 g).

2.2.1. Characterization details of [Rh(COD)($^{Ph}PN^{H}P$)]Cl (**2**)

IR (ν(NH)): 3370 cm−1. HRMS: *m*/*z* = 652.1759 [M]+ (calcd *m*/*z* for $C_{36}H_{41}NP_2Rh$ = 652.1769).

Elemental analysis for $C_{36}H_{41}NP_2ClRh$: Calcd: C, 62.84; H, 6.01; N, 2.04; Found: C, 59.87; H, 5.77; N, 1.99. The discrepancy could be attributed to oxidation of phosphine while weighing the sample in air for analysis (calcd for $C_{36}H_{41}NP_2ClRh\cdot O_2$: Calc: C, 60.05; H, 5.74; N, 1.95).

2.3. Synthesis of [$IrH_2Cl(^{Ph}PN^{H}P)$] (3)

[Ir(COD)($^{Ph}PN^{H}P$)]Cl (0.486 g, 0.715 mmol) was dissolved in 1,4-dioxane (30 mL) in a Parr reaction vessel (30 mL). The reaction setup was purged with H_2 before pressurizing the reactor with 10 bar of H_2. Subsequently, the reaction was stirred at 70 °C for 16 h. Then the solution was filtered over Celite, concentrated to about 5 mL, addition of *n*-hexane gave a colorless precipitate which was washed further with more *n*-hexane (3 × 10 mL) and then dried in vacuo. Complex **3** was isolated as a colorless solid. Yield: 70% (0.336 g).

2.3.1. Characterization details of [$IrH_2Cl(^{Ph}PN^{H}P)$] (**3**)

IR (ν(NH)): 3386 cm−1. HRMS: *m*/*z* = 636.1465 [M−Cl]+ (calcd *m*/*z* for $C_{28}H_{31}NP_2Ir$ = 636.1561).

Elemental analysis for $C_{28}H_{31}NP_2ClIr$: Calcd: C, 50.11; H, 4.66; N, 2.09; Found: C, 50.05; H, 4.749; N, 2.12.

2.4. Synthesis of [$RhH_2Cl(^{Ph}PN^{H}P)$] (4)

The synthetic procedure of [$RhH_2Cl(^{Ph}PN^{H}P)$] **4** is similar to that of complex **3** except that [Rh(COD)($^{Ph}PN^{H}P$)]Cl (0.200 g, 0.290 mmol) was used as the starting material. Complex **4** was isolated as a pale brown colored solid. Yield: 60% (0.100 g).

2.4.1. Characterization details of [$RhH_2Cl(^{Ph}PN^{H}P)$] (**4**)

IR (ν_{NH}): 3410 cm^{-1}. HRMS: *m*/*z* = 544.0830 [M−(Cl + H_2)]$^+$ (calcd *m*/*z* for $C_{28}H_{29}NP_2Rh$ = 544.0830).

Elemental analysis for $C_{28}H_{31}NP_2ClRh$: Calcd: C, 57.80; H, 5.37; N, 2.41; Found: C, 57.53; H, 5.24; N, 2.29.

2.5. In-situ characterization of [IrH_2(PhPNP)] complex (5) {PNP = −N-($CH_2CH_2PPh_2$)$_2$}

Inside a glove box, [$IrH_2Cl(^{Ph}PN^{H}P)$] complex (0.019 g, 0.028 mmol) and KOtBu/LiN($SiMe_3$)$_2$ (0.014 g, 0.120 mmol/0.008 g, 0.048 mmol) were suspended in C_6D_6 (0.6 mL) in a vial. The reaction mixture was shaken for few minutes. The colorless solution turned dark yellow. The clear solution was transferred to a NMR tube and spectra were acquired. Complex **5** was characterized only in solution due to its instability during isolation.

Characterization details of [IrH_2(PhPNP)] (**5**): 1H (C_6D_6, 293 K): −20.10 (t, *J*(H,P_{cis}) = 9 Hz, 1H, Ir–*H*), 2.69 (m, 4H, NCH_2), 2.88 (m, 2H, PCH_2), 3.49 (m, 2H, PCH_2), 7.01–8.09 (m, 20H, Ph).

31P (C_6D_6, 293 K): 53.89 (s).

2.6. Synthesis of [$IrH_3(^{Ph}PN^{H}P)$] (6)

[$IrH_2Cl(^{Ph}PN^{H}P)$] complex (0.418 g, 0.623 mmol) and KOtBu (0.278 g, 1.69 mmol) were taken together in a Parr hydrogenation reaction vessel. Then, THF (10 mL) was added under H_2 atm. The reaction flask was purged with H_2 before pressurizing the vessel to 10 bar. Then, the reaction contents were heated to 50 °C for 12 h. The reaction mixture was cooled to 298 K and filtered through Celite to remove KCl. Solvent was removed under vacuum. The yellow solid was washed with *n*-hexane (3 × 10 mL) and dried under vacuum. Complex **6** was isolated as a pale yellow solid. Yield: 81% (0.322 g).

From the NMR spectra, it was evident that the mer (**6a**) and fac (**6b**) isomers were formed in 50:50 ratio respectively.

Characterization details of [$IrH_3(^{Ph}PN^{H}P)$] (**6**):

IR (ν, cm^{-1}): 3370 (NH), 2090 (Ir–H). HRMS: 632.1193 {(M^+-($H+2H_2$).

Elemental analysis: for $C_{28}H_{32}NP_2Ir\cdot KCl$: Calcd: C, 47.28; H, 4.53; N, 1.97; Found: C, 46.88; H, 4.78; N, 1.86.

2.7. Synthesis of [$IrH_2(\eta^1$-O–C(O)H)($^{Ph}PN^HP$)] (7)

[$IrH_3(^{Ph}PN^HP)$] complex (0.020 g, 0.031 mmol) was stirred under CO_2 (1 atm) for 12 h at room temperature in THF (5 mL). The yellow colored solution paled down. The volume of the solvent was reduced by purging CO_2 through the solution before acquiring the NMR spectra. Attempts to isolate complex **7** were not successful because of its instability in the solid state.

2.8. Catalytic hydrogenation of CO_2

A general procedure for the catalytic hydrogenation of CO_2 is described here. Catalyst [$IrH_3(^{Ph}PN^HP)$] (0.006 g, 9.42 μmol) was weighed inside the glove box and transferred to a 25 mL Parr reactor vessel. Then, a small amount of THF (1 mL) and an aqueous solution of base were added (2–4 mL, 2–4 mmol). Finally, the reactor was pressurized with CO_2 (7 bar) followed by H_2 (7 bar) to a total pressure of 14 bar (1:1). The reaction parameters such as temperature (T (°C)) and time (t (h)) were set as summarized in Table 3 (S.M). Upon reaction completion, H_2O and THF were removed under vacuum. Then, D_2O was added to the reaction mixture and it was analyzed using ^1H and ^{13}C NMR spectroscopy.

2.9. General procedure for hydrogenation of carbonyl and imine substrates

[$IrH_3(^{Ph}PN^HP)$] (0.005 g, 7.85 μmol) was transferred to a 25 mL Parr reaction vessel inside a glove box. Then, substrate (7.85 mmol) and 10 mL of MeOH were added. The reaction contents were purged with H_2(g) for few minutes. The reaction mixture was stirred at 50 °C for 6–9 h (Table 4). Upon reaction completion, it was allowed to cool to 298 K and the solvent was removed under vacuum. The crude contents were passed through silica column to remove the catalyst and eluted with EtOAc/pet ether. The sample was analyzed by NMR spectroscopy and GC-MS (S.M.).

Table 2
Important bond length (Å) and bond angle (°) parameters for [$IrH_2Cl(^{Ph}PN^HP)$] (**3**) and [$IrH_3(^{Ph}PN^HP)$] (**6**).

	3	6
M–N(1)	2.15 (5)	2.201 (3)
M–P(1)	2.248 (17)	2.245 (10)
M–P(2)	2.274 (17)	2.245 (10)
M–/Cl(1)/H	2.478 (14)	1.61 (12)
M–H(1)	1.60 (4)	1.54 (4)
M–H(2)	1.90 (3)	1.51 (4)
N(1)–M–P(1)	84.60 (13)	84.36 (9)
P(1)–M–P(2)	167.25 (6)	166.29 (4)
N(1)–M– H(1)	165.17 (10)	178.31 (15)
H(2)–Ir–Cl/H(1)	173.31 (10)	175.64 (2)

Table 3
Optimization of reaction conditions for the catalytic hydrogenation of CO_2.

$$H_2 + CO_2 \xrightarrow[\substack{1\ M\ KOH_{(aq)}\\ T°C,\ t\ h}]{cat\ (0.2\ mol\ \%)} HCOOK \quad (3)$$

Sl No	T (°C)	t (h)	Aq. Base (1M)	TON
1	25	19	KOH	144
2	25	30	LiOH	66
3	45	36	LiOH	96
4	50	15	KOH	122
5	65	24	NaOH	65
6	65	24	LiOH	50
7	65	31	KOH	72
8	80	42	KOH	101
9 a	100	14	KOH	144
10	100	15	KOH	141

In all the cases, 1 mL of THF was added to solubilize the catalyst; a [$IrH_2Cl(^{Ph}PN^HP)$] complex was used as a catalyst. TON = No of moles of product formed/moles of catalyst. The calculated TON is the average of two runs.

2.10. X-ray crystal structure determination of complexes [Ir(COD)($^{Ph}PN^HP$)]Cl (1), [$IrH_2Cl(^{Ph}PN^HP)$] (3), [$RhH_2Cl(^{Ph}PN^HP)$] (4) and [$IrH_3(^{Ph}PN^HP)$] (6)

Colorless crystals of [Ir(COD)($^{Ph}PN^HP$)]Cl (**1**) complex was obtained by slow diffusion of hexane into a concentrated CH_2Cl_2 solution at 280 K. Colorless crystals of [$IrH_2Cl(^{Ph}PN^HP)$] (**3**), [$RhH_2Cl(^{Ph}PN^HP)$] (**4**) and yellow crystals of [$IrH_3(^{Ph}PN^HP)$] (**6**) complex were obtained from their THF solutions upon standing at 298 K. A single crystal suitable for diffraction study was chosen after careful examination under a microscope. The crystal was coated with paraton oil and mounted. Data was collected at 100/160 K. The unit cell parameters and intensity data were collected using a Bruker SMART APEX CCD diffractometer equipped with a fine focus Mo-K_α X-ray source. The SMART software was used for data acquisition and the SAINT program was used for data reduction [20]. The empirical absorption corrections were made using SADABS program [21]. The structure was solved using SHELX program [22]. All non-hydrogen atoms were located by difference Fourier map and refined anisotropically. The Ir–H and N–H hydrogen atoms were located in the difference Fourier map and refined isotropically. Other relevant data for structure refinement are summarized in the S.M.

3. Results and discussion

3.1. Synthesis and characterization of [$IrH_3(^{Ph}PN^HP)$] complex (6)

The [$IrH_3(^{Ph}PN^HP)$] complex (**6**) was synthesized as shown in Scheme 1. Treatment of [MCl(COD)]$_2$ {M = Ir, Rh} precursor complex with pincer ligand HN-($CH_2CH_2PPh_2$)$_2$ {$^{Ph}PN^HP$} in THF gave [M(COD)($^{Ph}PN^HP$)]Cl {M = Ir (**1**), Rh (**2**)} complexes in excellent yields, 86 and 91%, respectively. The allylic and the vinylic protons of Ir-COD fragment appear at 1.43 (br s) and 3.92 (br s) ppm respectively, in the ^1H NMR spectrum. Further, cooling the solution of complex **1** below 243 K, resulted in two different sets of signals for the allylic and the vinylic protons of COD moiety, respectively (S.M.). The N–H hydrogen signal was noted downfield at 8.18 (br s) ppm suggesting that there could be possible N–H···Cl interaction. In the IR spectrum, a broad band at 3370 cm^{-1} further supports hydrogen bonding interaction in this complex. Similar spectral features were noted for the Rh analogue. The $^{Ph}PN^HP$ ligand appeared at 15.00 (s) and 36.71 (d) ppm, respectively for complexes **1** and **2** in the ^{31}P NMR spectra. The ^1J(Rh,P) was found to be 120 Hz. The [Rh(COD)($^{Ph}PN^HP$)]Cl (**2**) complex was found to be extremely air sensitive whereas, the iridium analogue **1**, air stable. The N–H in [M(COD)($^{Ph}PN^HP$)]Cl complexes readily get deprotonated by Et_3N to form neutral complexes [M(COD)(PhPNP)] {M = Ir (**1a**), Rh (**2a**); PhPNP = –N($CH_2CH_2PPh_2$)$_2$} respectively along with the formation of Et_3NHCl. Previously, Don Tilley et al. reported the synthesis of [Ir(COD)(PNP)]Cl complex via reaction of [Ir(COD)Cl]$_2$ with PNP ligand having a rigid spacer (PNP = HN(2-PPh_2-4-Me-C_6H_3)$_2$) in toluene [23]. During the preparation of this manuscript, Casado et al. reported the synthesis and structural characterization of [Ir(COD)($^{Ph}PN^HP$)]Cl (**1**) complex [12].

Reaction of [M(COD)($^{Ph}PN^HP$)]Cl {M = Ir (**1**), Rh = (**2**)} complex with H_2 (10 bar) at 70 °C in THF/1,4-dioxane solvent resulted in the oxidative addition of H_2 to form the *cis*-dihydride [$MH_2Cl(^{Ph}PN^HP)$] {M = Ir (**3**), Rh (**4**)} complex. During the course of the reaction, COD gets hydrogenated into cyclooctane. Complexes **3** and **4** were isolated in moderate yields, 70 and 60% respectively. The Ir–H

Table 4
Hydrogenation of carbonyl and imine substrates using either [IrH_3(PNHP] (**6**) or [$IrH_2Cl(^{Ph}PN^HP)$] (**3**)/KOtBu as a catalyst.

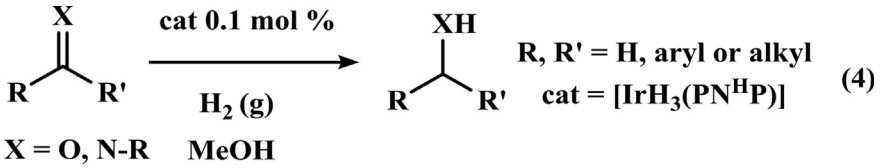

Sl No	substrate	Product	% conversion	t (h)
1a	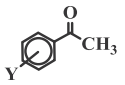	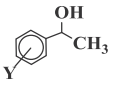	> 99	5-9
	Y = H, OMe, Cl, NO_2			
2	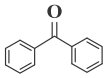	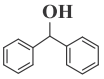	75	6
3		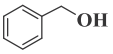	> 99	6
4			> 99	6
5			> 99	6
6			74	6
7b	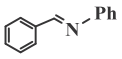	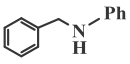	31	6
8c	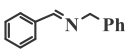	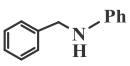	49	6
9	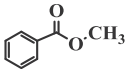	No reaction	-	-
10		No reaction	-	-

Reaction conditions: (a) Y = NO2, only 10% conversion was noted at H_2 (20 bar), 50 °C, 6 h in MeOH. (b) S:C ratio is 400:1 (c) The substrate to catalyst ratio was 1000:1 for all substrates except imines (400:1). The products were isolated through silica gel column chromatography (EtOAc/pet ether). All the reactions were repeated twice.

hydrogen signals were noted at −23.98 (td) and −19.04 (td) ppm with cis *J*(H,P) = 16 Hz in the ^{1}H NMR spectrum of **3**. The mutual coupling constant between the hydrides was found to be 7.5 Hz. Whereas, in the case of [$RhH_2Cl(^{Ph}PN^HP)$] complex **4**, the hydride signals appeared at −18.74 (m) and −14.86 (m) ppm with *J*(H,P_{cis}) of 16 Hz and ^{2}*J*(H,H) of 9 Hz in the ^{1}H NMR spectrum. Upon ^{31}P decoupling, the *J*(Rh,H) was found to be 28 Hz (S M.). The origin of the difference in hydride chemical shifts between Ir–H and Rh–H could be traced to the electronic structure of 5d vs 4d metal center [24]. The N–H hydrogen signal appeared at 4.19 (t) and 4.30 (t) ppm for complexes **3** and **4,** respectively. In the ^{31}P NMR spectrum, the $^{Ph}PN^HP$ ligand appeared at 26.31 (s) and 49.89 (d) ppm, respectively, for complexes **3** and **4**. The *J*(Rh, P) coupling constant was found to be 120 Hz for complex **4**. In the IR spectrum, a broad band was noted at 3386–3410 cm^{-1} for these complexes indicating hydrogen bonding interactions between N–H···Cl (S.M). The rhodium complexes are highly air sensitive whereas, the iridium analogues are air stable. Complex **3** could also be synthesized by the reaction of [$IrCl(COE)_2]_2$ with the $^{Ph}PN^HP$ ligand under H_2 (10 bar).

The analogous Ir complex [$IrH_2Cl(^iPrPN^HP)$] {$^iPrPN^HP$ = HN-($CH_2CH_2P^iPr_2)_2$} was synthesized by reacting $[Ir(COE)_2Cl]_2$ with $HN(CH_2CH_2P^iPr_2)_2$ in ^{i}PrOH at 80 °C [6]. Iluc and co-workers reported the formation of [IrH_2Cl(PNP)] {PNP = N-di(2-diisopropylphosphine-4-methylphenyl-*O*-tolylamine)} complex via reaction of $[Ir(COD)Cl]_2$ with PNP ligand under H_2 atm. The PNP ligand has a rigid backbone based on arene moiety and the nitrogen is substituted by tolyl (tolyl = $C_6H_4CH_3$) moiety [25]. Similarly, Goldman et al. reported the synthesis of [(tBufurPOP)RhH_2Cl] {tBufurPOP = 2,5-bis((di-*tert*-butylphosphino)methyl)furan} complex through reaction of $[Rh(NBD)Cl]_2$ (NBD = norbornadiene) with tBufurPOP ligand in toluene under 1 atm of H_2 at 110 °C [26].

Reaction of [$IrH_2Cl(^{Ph}PN^HP)$] (**3**) complex with excess KOtBu/$LiN(SiMe_3)_2$ in C_6D_6/THF-d_8 resulted in the formation of a highly unstable 16-electron amido dihydride complex [IrH_2(PhPNP)] (PNP = $-N(CH_2CH_2PPh_2)_2$) (**5**) via elimination of KCl and tBuOH/LiCl and $HN(SiMe_3)_2$ respectively. A single hydride signal was noted at −20.10 (t) with a *J*(H,P_{cis}) of 10 Hz in the ^{1}H NMR spectrum. The ^{31}P NMR spectrum is comprised of a signal at 53.90 (s) ppm which

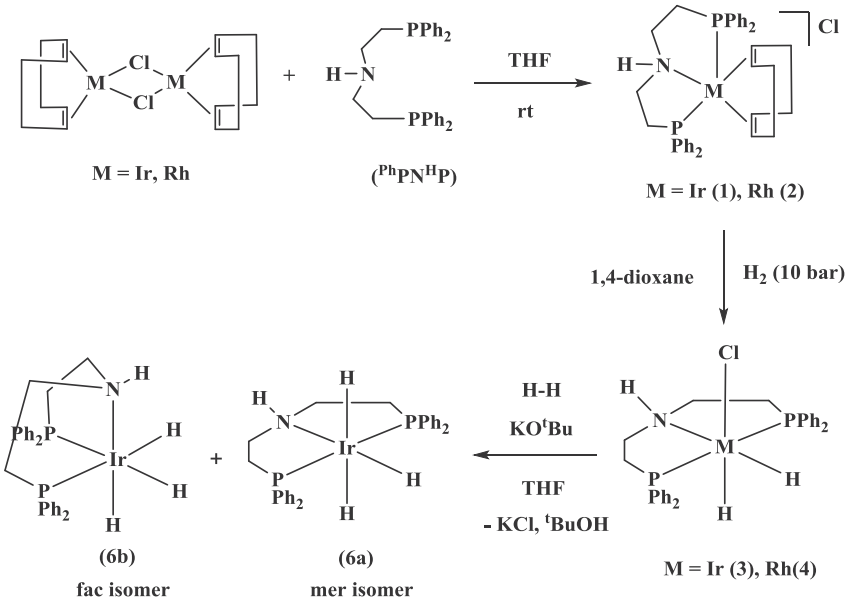

Scheme 1. Synthetic route for the preparation of [$IrH_3(^{Ph}PN^HP)$] complex (**6**).

is significantly upfield shifted compared to the starting material **3**. Based on the NMR spectral characteristics, the geometry of complex **5** could be described as a trigonal bipyramid. The intermediate [IrH_2(PNP)] (**5**) is too unstable to be explored for further reactions. On the other hand, a related complex [$IrH_2(^{i}PrPNP)$] (^{i}PrPNP = –N-($CH_2CH_2P^{i}Pr_2)_2$) where the phosphine ligand bears isopropyl substituents has been isolated, suggesting the role of steric and electronic factors imparted by isopropyl substituents in stabilizing 16-electron species [6].

The iridium amido dihydride complex [IrH_2(PhPNP)] (**5**) reacts rapidly with H_2 (6–10 bar) to afford the iridium trihydride complex [$IrH_3(^{Ph}PN^HP)$] (**6**) wherein H_2 is added across the Ir–N bond via 1,2-addition [27]. Fryzuk and his co-workers found that H_2 adds across the Ir–N bond in [IrH_2(PNP)] {PNP = –N($SiMe_2CH_2PPh_2)_2$} system to form *H*–N–Ir–*H* motif in an iridium amine trihydride complex [IrH_3(PNHP)] {PNP = HN($SiMe_2CH_2PPh_2)_2$}. Later, 1,2-addition reaction was observed in case of a few other systems based on Re and Ru pincer complexes [28]. It is now recognized as an important mode of bond activation in catalysis [29]. In contrast, the reaction of [$IrH_2(\kappa^3$-PNN)] {PNN = $tBu_2PC_2H_4NC_2H_4NEt_2$} complex in which the pincer arms are unsymmetrical with H_2 did not result in the formation of the anticipated trihydride complex, [$IrH_3(\kappa^3$-PN^HN)]. Instead, the presumed transient trihydride quickly dimerizes into a bridging hydride complex [$IrH_2(\kappa^2$-PN^HN)]$_2(\mu$-H)$_2$ suggesting subtle electronic factors in stabilizing the trihydride systems [30]. During the course of investigation of chiral N-alkyl pincer ligands for hydrogenation reactions, Bianchini et al. isolated a facial trihydride complex [IrH_3(PNRP)] (PNP = CH_3CH_2CH(Me) –N($CH_2CH_2PPh_2)_2$, R = –CH(Me)CH_2CH_3) via reaction of [Ir(COD)(H)(PNP)] with H_2 at room temperature [31].

The iridium trihydride [$IrH_3(^{Ph}PN^HP)$] (**6**) complex exists as two isomers: meridional (mer) and facial (fac), in the latter, the mutual trans arrangement of the strong trans influencing hydride ligands is avoided. From the ^{1}H NMR spectrum, these two isomers were found to be in a 50:50 ratio. Eight sets of distinct 'CH_2' signals in the range of 1.72–3.45 ppm were observed in the ^{1}H NMR spectrum for both mer and fac isomers, respectively. The ^{1}H NMR spectrum of the mer isomer **6a** shows two distinct hydride signals with identical triplet of doublet (td) pattern at –10.87 and –10.65 ppm (td) for the *trans* arrangement Ir–H moiety. The two trans hydrides were not equivalent. The coupling constants of J(H,P_{cis}) of 18.5 Hz and J(H,H) of 5 Hz were found. For the fac-isomer (**6b**), the hydride signals appear as a doublet of doublet pattern (dd) centered at –10.35 ppm with J(H,P_{trans}) of 120 Hz and J(H,P_{cis}) of 17 Hz. The signal of the hydride trans to N appeared as a multiplet at –19.39 and –19.52 ppm for mer and fac isomers, respectively. The N–H signal was noted at 5.26 (s) and 6.31 (t) respectively for the fac and mer isomers (S.M.) in the ^{1}H NMR spectrum. The $^{Ph}PN^HP$ ligand appeared at 31.89 (s) and 27.43 (s) ppm for *fac* and *mer* isomers of [$IrH_3(^{Ph}PN^HP)$] (**6**), respectively in the ^{31}P NMR spectrum. A broad band at 3370 cm^{-1} in the IR spectrum suggests the presence of hydrogen bonding in complex **6.**

3.2. X-ray crystal structures

ORTEP views of crystal structures of complexes **3** and **6** are shown in Fig. 1. The crystal structures of [Ir(COD)($^{Ph}PN^HP$)]Cl (**1**)

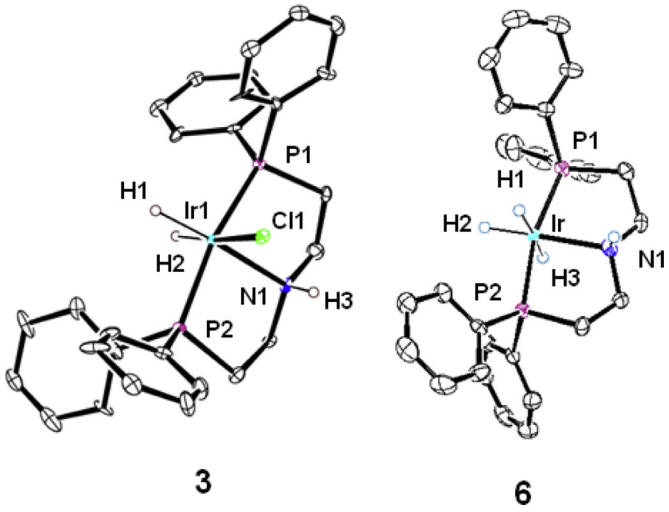

Fig. 1. ORTEP views of [$IrH_2Cl(^{Ph}PN^HP$] (**3**) and [$IrH_3(^{Ph}PN^HP$] (**6**) complexes shown at 50% ellipsoid probability level. All hydrogen atoms were omitted for clarity except Ir–H and N–H.

and [$RhH_2Cl(^{Ph}PN^HP)$] (**4**) complexes and the ball and stick packing of all the structures have been deposited in the S.M. In all of the structures, we were able to locate the hydrogen atoms bound to iridium and nitrogen from the difference Fourier maps and refined freely. The important bond lengths and bond angles of these complexes have been summarized in Table 2. Complex **1** was crystallized in CH_2Cl_2/*n*-hexane solvent system. Casado et al. recently reported the structural characterization of complex **1** via crystallization in acetone/diethyl ether [12]. In the crystal lattice two CH_2Cl_2 molecules were found which facilitates extensive hydrogen bonding network in the solid state. The structural parameters of complex **1** compare fairly well with reported structure except marginal difference in the torsion angles of the Ir-COD fragment (C8–C1–C2–C3 and C4–C5–C6–C7) [12].

$MH_2Cl(^{Ph}PN^HP)$] {M = Ir (**3**), Rh (**4**)} complexes crystallize in triclinic (P-1) and monoclinic ($P2_1/c$) crystal systems, respectively. These complexes adopt a slightly distorted octahedral structure. The bond angles P(1)-M(1)-P(2) and N(1)-M(1)-H(1) are in the range of 165.26–166.97° and 175.40–178.67°, respectively. The ligand rearranges to meridional geometry as compared to facial arrangement in the starting complexes **1** and **2**. One hydrogen atom was located trans to chloride and the other was located trans to the nitrogen atom. Additionally, extensive intra- (2.840 Å) and inter-molecular (2.515 Å) hydrogen bonding interactions between N–H···Cl were found. The metrical parameters of complex [$IrH_2Cl(^{Ph}PN^HP)$] are comparable to the [$IrH_2Cl(^{i}PrPN^HP)$] analogue 6. The bond distances and bond angles in [$RhH_2Cl(^{Ph}PN^HP)$] (**4**) are comparable to those of [(tBuXanPOP)RhH_2Cl] (tBuXanPOP = 4,5-bis(di-tertbutylphosphino)-9,9-dimethyl-9H-xanthene) complex [26].

[$IrH_3(^{Ph}PN^HP$] (**6**) complex crystallizes in monoclinic crystal system in $P2_1/c$ space group. The structure shows deviations from an ideal octahedral geometry. The P(1)-Ir(1)-P(2) and N(1)-Ir(1)-H(2) bond angles are 166.28 (4)° and 178.5 (15)°, respectively. The $^{Ph}PN^HP$ pincer ligand is arranged in a meridional geometry and the other three positions are taken up by hydrogen atoms. Two hydrogen atoms were located mutually *trans* to one another and the other hydrogen was located *trans* to the nitrogen donor. In the crystal packing weak intra- (2.691 Å) and inter-molecular (2.158 Å) N–H···H–Ir dihydrogen bonding interactions were evident. Dihydrogen bond is an intriguing type of hydrogen bond where M–H (M = transition metal/main group element) acts an acceptor and X–H (N, O) acts as a donor to constitute M–H···H–X interaction [32]. The strength of this interaction was estimated to be in the range 3–7 kcal/mol. Dihydrogen bonding has been recognized to play an important role in homogeneous catalysis where bi-functional/metal-ligand cooperative mechanism is involved [33].

It must be noted that the crystal structure of the catalytically active relevant iridium trihydride complexes [IrH_3(PNHP)] and {PNHP = HN-($CH_2CH_2P^iPr_2$)$_2$ and HN($SiMe_2CH_2PPh_2$)$_2$} has not been previously reported [34]. However, crystal structure of iridium trihydride [IrH_3(PNP)] (PNP = lutidine based pincer scaffold) complex supported by pyridine derived pincer ligands have been reported [35]. Compared to complex **6**, Ir–N (2.110(7) Å) bond distance is shorter and the Ir–P (2.252(2) Å) bond distance is longer in [IrH_3(PNP)] (PNP = lutidine based pincer scaffold). The P(1)–Ir–P(2) bond angle of 167.43 (8)° in [IrH_3(PNP)] (PNP = lutidine based pincer scaffold) is comparable to that in complex **6**. In the [IrH_3(PNP)] (PNP = lutidine based pincer scaffold) complex, the pincer motif was found to adopt planar arrangement whereas in complex **6**, the pincer moiety is non-planar. This is attributed to the 'CH_2' spacer in the $^{Ph}PN^HP$ ligand.

3.3. Reaction of [$IrH_3(^{Ph}PN^HP)$] (6) with CO_2

Reaction of the iridium trihydride complex [$IrH_3(^{Ph}PN^HP$)] (**6**) with CO_2 (1 atm) under ambient conditions lead to the formation of the formate derivative [$IrH_2(\eta^1$-OC(O)H)($^{Ph}PN^HP$)] (**7**) via insertion of CO_2 into the Ir–H bond (eq 2). The ^{1}H NMR spectrum of complex **7** is comprised of two hydride signals at −17.97 (td) and −27.07 (m) ppm with J(H,P_{cis}) of 13.5 Hz. The coupling between the inequivalent hydrides was found to be J(H,H) = 7 Hz. The signal for the formate moiety *H*COO− was found at 9.08 (t) ppm with J(H,H) = 10 Hz. The N–H signal was seen in the downfield region as a broad singlet at 8.08 ppm. The ^{31}P NMR spectrum shows a signal at 31.63 ppm for the $^{Ph}PN^HP$ ligand. The carbonyl carbon of the formate group appears at 172.16 ppm in the ^{13}C NMR spectrum. These spectral characteristics are similar to those of other reported complexes. For example, reaction of *trans*-[$ReH_2(NO)(^{i}PrPN^HP$)] with CO_2 led to its facile insertion into the Re – H bond to form *trans*-[$ReH(O_2CH)(NO)(^{i}PrPN^HP$)] [36]. Similarly, Bernskoetter et al. reported the formation of a formate complex [$FeH(\eta^1$-OC(O)H)(CN-R′)($^{i}PrPN^HP$)] {R' = 2,6-dimethoxyphenyl, 4-methoxyphenyl} via reaction of an unstable *trans*-[FeH_2(CN-R')($^{i}PrPN^HP$)] complex with CO_2 (1 atm). The Fe-formate complex decomposed slowly at room temperature in few hours. In addition to Fe-formate complex, few other unassigned products were noted in this reaction [37]. Attempts to isolate complex **7** were not successful because of its instability in the solid state.

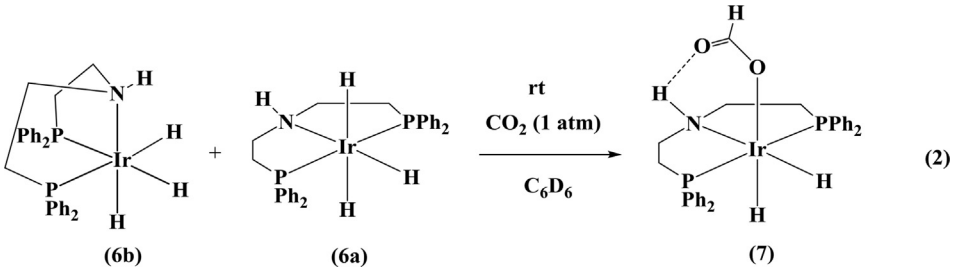

3.4. Catalytic hydrogenation of CO_2

Catalytic hydrogenation of CO_2 was carried out at a total pressure of 14 bar of H_2 and CO_2 (1:1) in the presence of 1 M base (aq). The performance of the catalyst [$IrH_3(^{Ph}PN^HP$)] **(6)** was evaluated under different conditions and the data are summarized in Table 3. In all cases small amount of THF was added to dissolve the catalyst. In the absence of the catalyst, formation of HCOOK was found to be negligible. An optimum catalyst loading of 0.2–0.4 mol % was used. The turn over number (TON) was calculated using $Me_3Si(CD_2)_2$-CO_2Na (sodium-3-trimethylsilylpropionate) as an internal standard

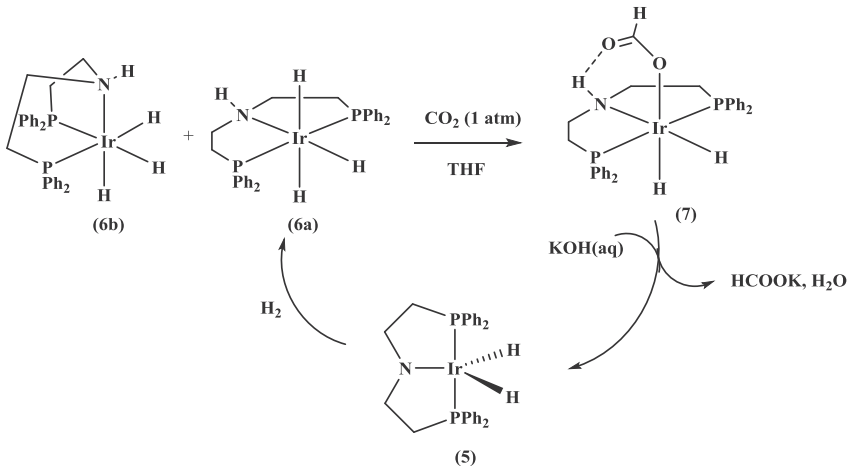

Scheme 2. Proposed catalytic cycle for the formation of HCOOK using [$IrH_3(^{Ph}PN^HP)$] complex (**6**) in 1 M KOH aqueous solution.

by ^1H NMR spectroscopy (S.M.). A maximum TON of 144 was obtained at room temperature using KOH as an aqueous base. The highest TOF of 47 h^{-1} was reached at 80 °C. Using KOH (aq) or NaOH (aq) as a base lead to the formation of $KHCO_3$ and $NaHCO_3$ along with HCOOK/HCOONa, respectively under the reaction conditions. This was confirmed by analysis of the reaction mixture using ^{13}C NMR spectroscopy (S.M.). Comparable TONs of 65 and 50 were achieved when $LiOH{\cdot}H_2O$ and NaOH were used as bases, respectively at 65 °C. Using [$IrH_2Cl(^{Ph}PN^HP)$] complex **3** as catalyst, a TON of 7 was achieved at room temperature in a duration of 24 h; however at 100 °C, a TON of 144 was reached in 14 h.

The relatively low TON, though under mild conditions of complex **6** could be attributed to the instability of the catalyst in aqueous KOH solution. Also, the relatively high electrophilicity of the metal complex compared to other reported complexes due to the presence of phenyl group on the phosphorus would also contribute to the low TON. Nozaki et al. reported the formation of HCOOK in 1 M KOH (aq) solution from H_2 and CO_2 promoted by [IrH_3(PNP)] (PNP = lutidine based pincer scaffold) catalyst with the highest TON and TOF of 350000 and 150000 h-1, respectively. The catalyst operates at 200 °C and 50 bar of total pressure of 1:1H_2 and CO_2 [35]. Hazari and co-workers investigated the role of secondary sphere interactions between N–H fragment of pincer ligand and the oxygen atom of formate moiety in M-*O*–C(*O*)H which facilitates the insertion of CO_2 into Ir–H bond in [$IrH_3(^iPrPN^HP)$] complex. The bifunctional behavior of the catalyst due to N–H···O–C(O)H–M interaction makes it a very active catalyst. This catalyst also operates at 185 °C and 55 bar of total pressure [5].

The proposed mechanism for the hydrogenation of CO_2 in 1 M base (aq) is outlined in Scheme 2. Attack of the nucleophilic *trans* Ir–H bond onto CO_2 in the first step leads to formation of the formate complex [$IrH_2(\eta1$-OC(O)H)$(^{Ph}PN^HP)$] (**7**) [38]. The formate complex [$IrH_2(\eta^1$-OC(O)H)$(^{Ph}PN^HP)$] (**7**) further gets stabilized by the secondary sphere interactions between the oxygen atom of formate group HC*OO*–Ir and N–H [5]. Evidence for this was obtained from ^1H NMR spectroscopy of a signal for the N–*H* moiety (δ 8.8 ppm). In the second step, reaction of the formate (**7**) complex with KOH results in the elimination of HCOOK with concomitant formation of a highly reactive amido dihydride complex [IrH_2(PhPNP)] (**5**) (PNP = $-N(CH_2CH_2PPh_2)_2$) and H_2O. Subsequently, H_2 adds across the Ir–N bond in the amido dihydride [IrH_2(PNP)] complex (**5**) to regenerate the catalyst [$IrH_3(^{Ph}PN^HP)$] (**6**), thus completing the catalytic cycle. The mechanism is supported by NMR spectral study of the catalytic cycle (S.M.). The plausible mechanism proposed here is closely related to the ones reported in the literature [39].

3.5. Catalytic hydrogenation of carbonyl and imine substrates

In addition to catalytic hydrogenation of CO_2, [$IrH_3(^{Ph}PN^HP)$] (**6**) complex acts as a catalyst for hydrogenation of polar organic substrates containing carbonyl and imine functionalities (Table 4). Reaction conditions were optimized using acetophenone as a model substrate (S.M.). A catalyst loading of 0.1 mol % was used. Acetophenone and its derivatives were hydrogenated completely at 50 °C with H_2(g) (10 bar) in 5–9 h. In case of *p*-nitroacetophenone only 10% conversion to the corresponding alcohol product was noted under similar conditions. Benzaldehyde and 2-butanone, were quantitatively reduced to benzyl alcohol and 2-butanol, respectively in 6 h at 50 °C. Benzophenone and tetralone were reduced to the corresponding alcohol products, respectively in 75%

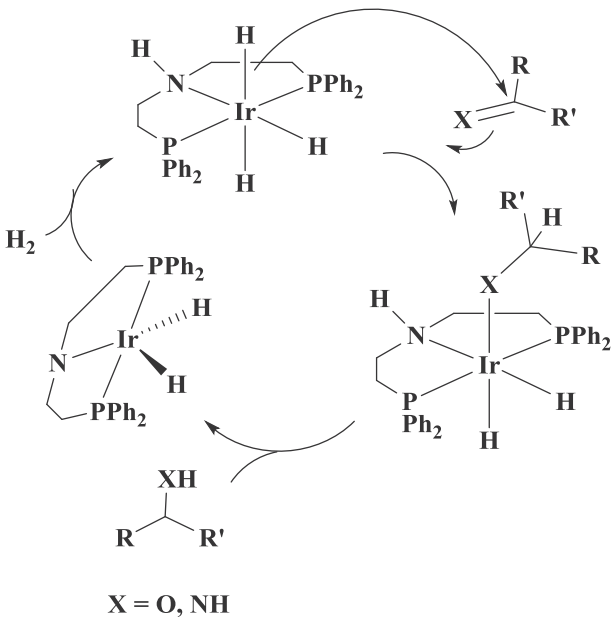

Scheme 3. Mechanism for the base-free hydrogenation of carbonyl and imine substrates.

conversion in 6 h at 50 °C. However, with increased reaction time (9 h, 60 °C), complete conversion was achieved. Moderate conversions were noted for the hydrogenation of N-benzylidene aniline and N-benzylidene benzylamine (49%) at much slower rates compared to carbonyl compounds under similar conditions. Styrene, 3-pentanone and methyl benzoate did not undergo hydrogenation under the reaction conditions (20 bar, 50 °C, 6 h) or even harsh conditions. The lack of hydrogenation of 3-pentanone compared to 2-butanone is attributed to its symmetrical nature and steric hindrance associated with it.

To date, there have been very few reports for the hydrogenation of carbonyl and imine substrates using iridium metal complexes as catalysts [40]. Base-free hydrogenation reactions using H_2(g) catalyzed by iridium hydride metal complexes are even more scarce.

Compared to transfer hydrogenation, direct hydrogenation using H_2(g) is considered to be a green route for industrial scale applications [41]. For example, Abdur-Rashid et al. reported direct hydrogenation (H_2 = 10 bar) of carbonyl substrates in MeOH at room temperature using [IrH_3(^{i}PrPN^{H}P)] complex [42]. The catalytic activity of [IrH_3(^{Ph}PN^{H}P)] (**6**) is comparable to that of [IrH_3(^{i}PrPN^{H}P)] complex under the given conditions. The substituents on phosphorus of the RPNHP pincer ligand (R = iPr vs Ph) have no influence on the reduction of carbonyl and imine compounds. Additionally, complex **6** also hydrogenates imines N-benzylidene aniline and N-benzylidene benzylamine (entries 7 and 8, Table 4). Claver et al. reported catalytic hydrogenation of imines using diorthometalated iridium phosphite complex [IrH(COD)P(OC_6H_2-2,4-tBu_2)$_2$(OC_6H_2-2,4-tBu_2)] at 30 bar H_2(g) at 40 °C in MeOH with a substrate to precatalyst ratio of 100:1 [43]. Herrera and co-workers reported hydrogenation of imines at 200 psi pressure of H_2(g) at 60 °C for 18 h with a S:C of 100:1 using [M(COD)(PPh_3)$_2$]PF_6 {M = Ir, Rh} [44]. Our attempts to employ [RhH_2Cl(^{Ph}PN^{H}P)] (**4**) complex as a catalyst for the hydrogenation of CO_2, carbonyl and imine substrates were not successful. This could be attributed to the lack of formation of an active catalyst, [RhH_3(^{Ph}PN^{H}P)] complex under the reaction conditions.

To elucidate the mechanism of the catalytic reaction, hydrogenation of acetophenone was investigated using NMR spectroscopy. Dissolution of [IrH_3(^{Ph}PN^{H}P)] (**6**) in MeOD-d_4 resulted in H–D exchange between MeO-D and Ir–H. Free H–D signal was noted at 4.60 ppm with J(H,D). = 43 Hz in the ^{1}H NMR spectrum (S.M.). The reaction of [IrH_3(^{Ph}PN^{H}P)] (**6**) with excess $PhCOCH_3$ was studied in toluene-d_8 (S.M.). Addition of $PhCOCH_3$ to complex **6** resulted in the formation of a new set of hydride signals at −16.38 and −18.54 ppm with J(H,P_{cis}) = 16 Hz and J(H,H) = 5 Hz Hz, respectively in the ^{1}H NMR spectrum. Additionally, the N–H signal was noted at 5.10 ppm. A signal at 30.70 ppm was noted in the ^{31}P NMR spectrum. Simultaneously, $PhCOCH_3$ was converted into $PhCH(OH)CH_3$ as noted by the appearance of signals in the ^{1}H and ^{13}C NMR spectra. This clearly suggests an inner sphere mechanism where Ir–H attacks Ph–⊖CO–CH_3 molecule to form Ir–*O*–C(H)R_2 species. Introducing H_2(g) (5 bar) into the sample regenerated the active hydrogenation catalyst, **6**. Though there was no evidence for the existence of [IrH_2(PhPNP)] (**5**) during the catalytic cycle, the formation of **6**, Ph*CH*(*OH*)CH_3, and the disappearance of N–H signal suggest its presence in the catalytic cycle. This is in contrast to the tentative mechanism proposed for the analogous [IrH_3(^{i}PrPN^{H}P] complex where a bi-functional outer sphere mechanism was suggested [6]. Kirchner et al. reported inner sphere type mechanism for the base assisted hydrogenation of ketones catalyzed by [Fe(PNP-^{i}Pr)(H)(CO)Br] {PNP-^{i}Pr = 2,6-diaminopyrine based ligand} complex; support for this was found in the form of an attack of Fe–H onto the carbonyl moiety in the catalytic cycle [45]. The widely accepted bifunctional mechanism could be much more prevalent in ruthenium complexes containing H–Ru–N–H motif compared to iridium analogues [46].

3.6. Catalytic hydrogenation of α,β-unsaturated ketones

Surprisingly, hydrogenation of 2-cyclohexen-1-one at room temperature resulted in a mixture of cyclohexanol (18%) and 3-methoxycyclohexanol (82%) in MeOH (S.M.). The identity of the products was established by ^{1}H and ^{13}C NMR spectroscopy and GC-MS analysis. 3-Methoxycyclohexanol exists as both *cis*- and *trans*-diastereomers. Similarly, hydrogenation of 2-cyclohexen-1-one in ethanol resulted in the formation of 3-ethoxycyclohexanol (85%) along with the formation of cyclohexanol (15%). However, in case of hydrogenation of 2-cyclohexen-1-one in isopropanol resulted a mixture of 2-cyclohexen-1-ol (17%) and cyclohexanol (44%). On the other hand, hydrogenation of 2-cyclohexen-1-one in THF gave exclusively cyclohexanol. All reactions were carried out for 24–36 h at room temperature. The detailed reaction conditions optimization are given in S.M. These results are in sharp contrast to the chemoselective reduction of the carbonyl group in α, β-unsaturated compounds catalyzed by [IrH_2Cl(^{i}PrPN^{H}P)]/KOtBu and [OsH_2(CO)(κ3-$PyCH_2NHC_2H_4NHPtBu_2$)] complexes [47].

The formation of 3-methoxy/3-ethoxy cyclohexanol under the reaction conditions suggests tandem Michael addition-hydrogenation type reaction. In general, Michael addition reactions could be catalyzed by Lewis acid catalysts such as Cu(OTf)$_2$, B(C_6F_5)$_3$, $AlCl_3$ etc. [48] We propose that the presence of phenyl groups on phosphorus could make the metal complex relatively acidic which results in the increased acidity of N–H of the pincer ligand. Casado and co-workers utilized the acidity of N–H in ^{Ph}PN^{H}P ligand in [Ir(COD)(^{Ph}PN^{H}P)]Cl complex to protonate 'OMe' group in [Ir(μ-OMe)(COD)]$_2$ [12]. We propose that complex **6** could behave as a Lewis acidic bifunctional catalyst which facilitates nucleophilic attack of MeOH at position 3 in 2-cyclohexen-1-one (Fig. 2). In the subsequent step, hydrogenation of Michael addition product 3-methoxycyclohexenone could lead to 3-methoxycyclohexanol. Lewis acid catalyzed Micheal-addition of α, β-unsaturated substrates were documented earlier [49]. Morris et al. studied tandem Michael addition-hydrogenation of 2-cyclohexen-1-one in benzene using *trans*-[RuH(η1-BH_4)((*S*)-Ppro)$_2$] {(*S*)-Ppro = (*S*)-2-(diphenylphosphinomethyl)pyrrolidine} as a catalyst and dimethylmalonate as a Michael donor. However, low yields were noted when the reaction was carried out EtOH or ^{i}PrOH [50].

4. Conclusions

A family of Ir and Rh complexes [M(COD)(^{Ph}PN^{H}P)]Cl {M = Ir (**1**), Rh (**2**), ^{Ph}PN^{H}P = HN($CH_2CH_2PPh_2$)$_2$}, [MH_2Cl(^{Ph}PN^{H}P)] {M = Ir (**3**), Rh (**4**)} and [IrH_3(^{Ph}PN^{H}P)] (**6**) were synthesized. All complexes were isolated in good yields and characterized by various analytical techniques. The [IrH_3(^{Ph}PN^{H}P)] (**6**) complex was found to be an active catalyst for the hydrogenation of CO_2 to HCOOK in 1M base (aq). Complex **6** was also found to be an active catalyst for the base-free hydrogenation of polar (carbonyl, 2-cylohexen-1-one, imines)

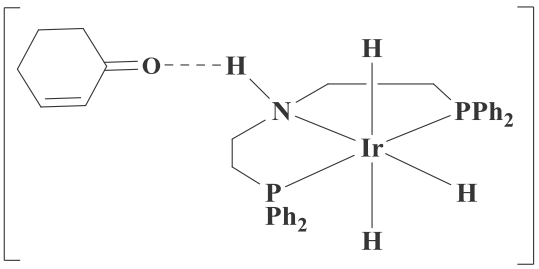

Fig. 2. Proposed structure of Lewis acidic nature of the bifunctional catalyst [[IrH_3(^{Ph}PN^{H}P)] (**6**) for the tandem Michael addition-hydrogenation reaction.

substrates. Additionally, Lewis-acid-catalyzed tandem Michael addition-hydrogenation was achieved for 2-cyclohexen-1-one in ROH solvent (R = Me, Et) using complex **6**.

Acknowledgements

We gratefully acknowledge financial support from Department of Science & Technology (Science & Engineering Research Board, SERB), of India. A Ramaraj acknowledges DST for a fellowship.

Appendix A. Supplementary data

Supplementary data to this article can be found online at https://doi.org/10.1016/j.jorganchem.2018.12.017.

References

[1] (a) K.A. Grice, Coord. Chem. Rev. 336 (2017) 78–95;
(b) M. Behrens, Angew. Chem. Int. Ed. 55 (2016) 14906–14908;
(c) S. Bontemps, Coord. Chem. Rev. 308 (2016) 117–130;
(d) M. Feller, E. Ben-Ari, Y. Diskin-Posner, D. Milstein, J. Coord. Chem. (2018). https://doi.org/10.1080/00958972.2018.1475662;
(e) L. Vaska, J. Mol. Catal. 47 (1988) 381–388;
(f) X. Yin, J.R. Moss, Coord. Chem. Rev. 181 (1999) 27–59;
(g) N.A. Tappe, R.M. Reich, V. D'Elia, F.E. Kuhn, Dalton Trans. (2018), https://doi.org/10.1039/c8dt02346h;
(h) M. Areta (Ed.), Carbon Dioxide as Chemical Feedstock, Wiley-VCH, Weinheim, 2010;
(i) M. Cokoja, C. Bruchkmeier, B. Rieger, W.A. Herrmann, F.E. Kuhn, Angew. Chem. Int. Ed. 50 (2011) 8510–8537;
(j) F. Fernandez-Alvarez, M. Iglesias, L.A. Oro, V. Polo, ChemCatChem 5 (2013) 3481–3494;
(k) J. Klankermayer, S. Wesslbaum, K. Beydoun, W. Leitner, Angew. Chem. Int. Ed. 55 (2016) 7296;
(l) R. Stichauer, A. Helmers, J. Bermer, M. Rohdenburg, A. Wark, E. Lork, M. Vogt, Organometallics 36 (2017) 839–848;
(m) W.H. Bernskoetter, N. Hazari, Eur. J. Inorg. Chem. 22–23 (2013) 4032–4041;
(n) S. Ramakrishnan, K. Waldie, I. Warnke, A.G.D. Crisci, V.S. Batista, R.M. Waymouth, C.E.D. Chidsey, Inorg. Chem. 55 (2016) 1623–1632;
(o) A.Z. Spentzos, C.L. Barnes, W.H. Bernskoetter, Inorg. Chem. 55 (2016) 8225–8233;
(p) C. Gunanathan, D. Milstein, Acc. Chem. Res. 44 (2011) 588–602;
(q) M. Vogt, M. Gargir, M.A. Iron, Y. Diskin-Posner, Y. Ben-David, D. Milstein, Chem. Eur J. 18 (2012) 9194–9197;
(r) J.F. Hull, Y. Himeda, W.H. Wang, B. Hashiguchi, R. Periana, D.J. Szalda, J.T. Muckerman, E. Fujita, Nat. Chem. 4 (2012) 383–388;
(s) K. Sordakis, A. Tsurusaki, M. Iguchi, H. Kawanami, Y. Himeda, G. Laurenczy, Chem. Eur J. 22 (2016) 15605–15608.
[2] N. Hazari, J.E. Heimann, Inorg. Chem. 56 (2017) 13655–13678.
[3] G.A. Olah, A. Goeppert, G.K. Surya Prakash, J. Org. Chem. 74 (2009) 487–498.
[4] (a) M. Asay, D. Morales-Morales, Top. Organomet. Chem. 54 (2016) 239;
(b) G. Van Koten, R.A. Gossage, The Previleged Pincer-metal Platform: Coordinated Chemistry & Applications, vol. 54, Springer, Berlin, 2016;
(c) C. Gunanathan, D. Milstein, Science 341 (2013) 1229712;
(d) M. Asay, D. Morales-Morales, Dalton Trans. 44 (2015) 17432–17447;
(e) S. Murugesan, K. Kirchner, Dalton Trans. 45 (2016) 416–439;
(f) H.A. Younus, W. Su, N. Ahmad, S. Chen, F. Verpoort, Adv. Synth. Catal. 357 (2015) 283–330;
(g) S. Werkmeister, J. Neumann, K. Junge, M. Beller, Chem. Eur J. 21 (2015) 1–26;
(h) D. Morales-Morales, C.M. Jensen, The Chemistry of Pincer Compounds, first ed., Elsevier, Amsterdam, 2007;
(i) M. Albrecht, G. van Koten, Angew. Chem. Int. Ed. 40 (2001) 3750–3781;
(j) M.E. van der Boom, D. Milstein, Chem. Rev. 103 (2003) 1759–1792;
(k) J.T. Singleton, Tetrahedron 59 (2003) 1837–1857;
(l) D. Benito-Garagorri, K. Kirchner, Acc. Chem. Res. 41 (2008) 201–213;
(m) S. Schneider, J. Meiners, B. Askevold, Eur. J. Inorg. Chem. 3 (2012) 412–429;
(n) N.A. Espinosa-Jalapa, S. Hernandez-Ortega, X.–F. Le Goff, D. Morales-Morales, J.–P. Djukic, R. Le Lagadec, Organometallics 32 (2013) 2661–2673.
[5] T.J. Schmeier, G.E. Dobereiner, R.H. Crabtree, N. Hazari, J. Am. Chem. Soc. 133 (2011) 9274–9277.
[6] Z.E. Clarke, P.T. Maragh, T.P. Dasgupta, D.G. Gusev, A.J. Lough, K. Abdur-Rashid, Organometallics 25 (2006) 4113–4117.
[7] S.E. Clapham, A. Hadzovic, R.H. Morris, Coord. Chem. Rev. 248 (2004) 2201–2237.
[8] R.H. Morris, Chem. Soc. Rev. 38 (2009) 2282–2291.
[9] R. Noyori, S. Hashiguchi, Acc. Chem. Res. 30 (1997) 97–102.
[10] J.M. Goldberg, G.W. Wong, K.E. Brastow, W. Kaminsky, K.I. Goldberg, D.M. Heinekey, Organometallics 34 (2015) 753–762.
[11] (a) M.M. Taqui Khan, B. Taqui Khan, S. Begum, J. Mol. Catal. 34 (1986) 9–18;
(b) M.M. Taqui Khan, B. Taqui Khan, Safia, K. Nazeeruddin, J. Mol. Catal. 26 (1984) 207–217.
[12] P. Hermosilla, P. Lopez, P. Garcia-Orduna, F.J. Lahoz, V. Polo, M.A. Casado, Organometallics 37 (2018) 2618–2629.
[13] D.F. Shriver, M.A. Drezdon, The Manipulation of Air Sensitive Compounds, second ed., Wiley, New York, 1986.
[14] W.L.F. Armarego, C.L.L. Chai, Purification of Laboratory Chemicals, fifth ed., Elsevier, London, 2003.
[15] J.L. Herde, J.C. Lambert, C.V. Senoff, Inorg. Synth. 15 (1974) 18–20.
[16] G. Giordano, R.H. Crabtree, Inorg. Synth. 19 (1979) 218–220.
[17] (a) N.A. Yakelis, R.G. Bergman, Organometallics 24 (2005) 3579–3581;
(b) A.A. Donopoulos, A.R. Wills, P.G. Edwards, Polyhedron 9 (1990) 2413–2418.
[18] M. Porchia, F. Tisato, F. Refosco, C. Bolzati, M. Cavazza-Ceccato, G. Bandol, A. Dolmella, Inorg. Chem. 44 (2005), 4766-4766.
[19] J. Clayden, N. Greeves, S. Warren, Organic Chemistry, second ed., 2014.
[20] SMART, SAINT, Version 6.22a, Bruker AXS, Madison, WI, 1999.
[21] (a) G.M. Sheldrick, SADABS, Version 2; Multiscan Absorption Correction Program, University of Gottingen, Gotingen, Germany, 2001;
(b) R.H. Blessing, Acta Crystallogr. A 51 (1995) 33.
[22] G.M. Sheldrick, SHELXL-97 Program for the Solution of Crystal Structures, University of Gottingen, Gotingen, Germany, 1997.
[23] E. Calimano, D.T. Tilley, Dalton Trans. 39 (2010) 9250–9263.
[24] P. Hrobarik, V. Hrobarikova, F. Meier, M. Repisky, S. Komorovsky, M. Kaupp, J. Phys. Chem. A 115 (2011) 5654–5659.
[25] S.P. Vilanova, V. Iluc, Organometallics 35 (2016) 2110–2123.
[26] M.C. Haibach, D.Y. Wang, T.J. Emge, K. Krogh-Jespersen, A.S. Goldman, Chem. Sci. 4 (2013) 3683–3692.
[27] M.D. Fryzuk, P. Macnell, Organometallics 2 (1983) 682–684.
[28] T.C. Wambach, M.D. Fryzuk, Inorg. Chem. 54 (2015) 5888–5896.
[29] H. Grutzmacher, Angew. Chem. Int. Ed. 47 (2008) 1814–1818.
[30] A. Choualab, A.J. Lough, D.G. Gusev, Organometallics 26 (2007) 5224–5229.
[31] (a) C. Bianchini, L. Glendenning, M. Perzzinin, G. Purches, F. Zanobini, E. Farnetti, M. Graziani, G. Nardin, Organometallics 16 (1997) 4403–4414;
(b) C. Bianchini, L. Glendenning, M. Perzzinini, G. Purches, F. Zanobini, E. Farnetti, M. Graziani, G. Nardin, Organometallics 16 (1997) 4403–4414.
[32] R.H. Crabtree, P.E.M. Siegbahn, O. Eisenstein, A.L. Rheingold, T.F. Koetzle, Acc. Chem. Res. 29 (1996) 348–354.
[33] N.V. Belkova, L.M. Epstein, O.A. Filippov, E. Shubina, Chem. Rev. 116 (2016) 8545–8587.
[34] M.D. Fryzuk, P.A. MacNeil, S.J. Rettig, J. Am. Chem. Soc. 109 (1987) 2803–2812.
[35] R. Tanaka, M. Yamashita, K. Nozaki, J. Am. Chem. Soc. 131 (2009) 14168.
[36] A. Choualeb, A.J. Lough, D.G. Gusev, Organometallics 26 (2007) 3509–3515.
[37] N.F. Smith, W.H. Bernskoetter, N. Hazari, B.Q. Mercade, Organometallics 36 (2017) 3995–4004.
[38] J. Li, K. Yoshizawa, Bull. Chem. Soc. Jpn. 84 (2011) 1039–1048.
[39] (a) R. Tanaka, M. Yamashita, L.W. Chung, K. Morokuma, K. Nozaki, Organometallics 30 (2011) 6742–6750;
(b) X. Yang, ACS Catal. 1 (2011) 849–854.
[40] G.P. Anderson, Topics in Organometallic Chemistry, Iridium Catalysis, 2010 (Berlin).
[41] J.G. De Vries, C.J. Elsevier, in: V.C.H. Wiley (Ed.), Handbook of Homogeneous Hydrogenation, 2006, pp. 1–3. Weinheim, Germany.
[42] X. Chen, W. Jia, R. Guo, T.W. Graham, M.A. Gullons, K. Abdur-Rashid, Dalton Trans. (2009) 1407–1409.
[43] R.B. Bedford, S. Costillion, P.A. Chaloner, C. Claver, E. Fernandez, P.B. Hitchcock, A. Ruiz, Organometallics 15 (1996) 3990–3997.
[44] V. Herrera, B. Munoz, M.V. Landaeta, J. Mol. Catal. Chem. 174 (2001) 141–149.
[45] N. Gorgas, B. Stoger, L.F. Veiros, E. Pittenauer, G. Allmaier, K. Kirchner, Organometallics 33 (2014) 6905–6914.
[46] (a) D. Gelman, S. Musa, ACS Catal. 2 (2012) 2456–2466;
(b) O. Eisenstein, R.H. Crabtree, New J. Chem. 37 (2013) 21–27;
(c) R.H. Morris, Dalton Trans. 47 (2018) 10809–10826;
(d) T. Ohkuma, H. Doucet, T. Pham, K. Mikami, T. Korenaga, M. Tevada, R. Noyori, J. Am. Chem. Soc. 120 (1998) 1086-1087. (e) K. Abdur-Rashid, A.J. Lough, R.H. Morris, Organometallics 19 (2000) 2655–2657;
(f) B.L. Conley, M.K. Pennington-Boggio, E. Boz, T.J. Williams, Chem. Rev. 110 (2010) 2294–2312.
[47] D. Spasyuk, C. Vicent, D.G. Gusev, J. Am. Chem. Soc. 137 (2015) 3743–3746.
[48] (a) A. Mekonnen, R. Carlson, Eur. J. Org. Chem. 8 (2006) 2005–2013;
(b) K. Ishihara, N. Hanaki, M. Funahashi, M. Miyata, H. Yamamoto, Bull. Chem. Soc. Jpn. 68 (1995) 1721–1730.
[49] S.K. Leitch, A. McCluskey, Synlett 5 (2003) 699–701.
[50] (a) R. Guo, R.H. Morris, D. Song, J. Am. Chem. Soc. 127 (2005) 516–517;
(b) R. Guo, X. Chen, C. Elpet, D. Song, R.H. Morris, Org. Lett. 7 (2005) 1757–1759.